analytical chemistry

pubs.acs.org/ac Article

Physicochemical Properties Predict Retention of Antibiotics in Water-in-Oil Droplets

Artur Ruszczak,[§] Paweł Jankowski,[§] Shreyas K. Vasantham, Ott Scheler,* and Piotr Garstecki*

Cite This: *Anal. Chem.* 2023, 95, 1574−1581 Read Online

ACCESS | Metrics & More | Article Recommendations | Supporting Information

ABSTRACT: Water-in-oil droplet microfluidics promises capacity for high-throughput single-cell antimicrobial susceptibility assays and investigation of drug resistance mechanisms. Every droplet must serve as an isolated environment with a controlled antibiotic concentration in such assays. While technologies for generation, incubation, screening, and sorting droplets mature, predictable retention of active molecules inside droplets remains a major outstanding challenge. Here, we analyzed 36 descriptors of the antibiotic molecules against experimental results on the cross-talk of antibiotics in droplets. We show that partition coefficient and fractional polar surface area are the key physicochemical properties that predict antibiotic retention. We verified the prediction by monitoring growth inhibition by antibiotic-loaded neighboring droplets. Our experiments also demonstrate that transfer of antibiotics between droplets is concentration- and distance-dependent. Our findings immediately apply to designing droplet antibiotic assays and give deeper insight into the retention of small molecules in water-in-oil emulsions.

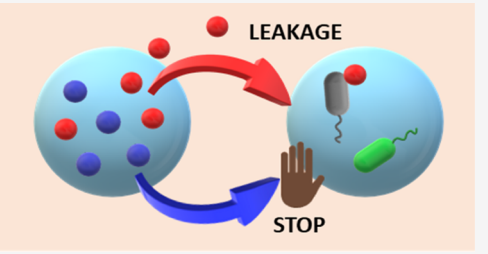

INTRODUCTION

Microfluidic droplet systems have recently been shown to demonstrate highly attractive analytical methods in antimicrobial susceptibility testing (AST) and in investigating antimicrobial resistance mechanisms. Microfluidics offers convenient methods for the generation of highly monodisperse droplets. Monodisperse aqueous droplets can serve as individual and isolated environments for microbial growth, thus allowing for high-throughput experimentation on thousands or millions of miniature incubation 'chambers'.[1−6] The key requirement and one of the major challenges in these experiments is to control and maintain the chemical composition of each droplet incubator. Enabling the development and applicability of droplet analytical systems to study bacterial response to antibiotics is important because of the global health breakdown caused by the rapid emergence of resistant pathogens.[7] Droplet methods promise a host of advantages over conventional AST methods, such as a multicomponent chemical environment or high-throughput population analysis with single-cell resolution.[8,9] All of these features make microfluidics suitable for characterization phenomena such as heterogeneity, responses of bacteria in complex consortia, or the influence of the inoculum effect.[10−12]

There are several possible physical mechanisms of the chemical escape from droplets: (i) diffusion to the oil phase, (ii) micelles or small ripening droplet formation, and (iii) transport through a bilayer membrane between two droplets touching each other (Figure 1).[13−19] Small molecules with a hydrophobic nature will more likely escape from aqueous phases into the oil phase. This possibly explains problems with the retention molecules commonly used in life sciences, like

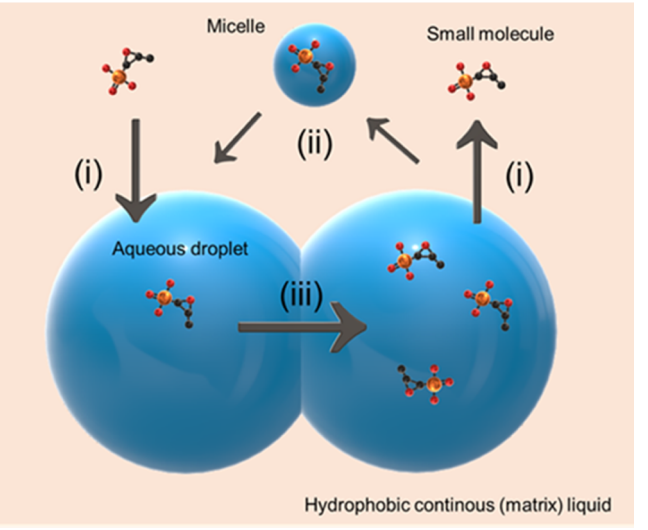

Figure 1. Possible mechanisms of chemical transport between droplets: (i) diffusion to the oil and transport from the oil to the droplet, (ii) small micelles and or detached satellites, and (iii) transport between membranes of touching droplets.

Received: October 20, 2022
Accepted: December 2, 2022
Published: January 4, 2023

https://doi.org/10.1021/acs.analchem.2c04644
Anal. Chem. 2023, 95, 1574−1581

fluorescein or resorufin.[20−22] Additionally, most of the droplet-based systems work on relatively high concentrations of surfactants (far over the critical micelle concentration—CMC). Together with the aging of emulsions, this can lead to the spontaneous formation of reverse micelles.[14,18]

The literature demonstrates that micelles, vesicles, or even tiny spontaneously formed droplets can work as vehicles for some molecules transporting them between droplets. The size of these spontaneously formed droplets can reach up to 100 nm.[14,17] Finally, emulsions possess a tendency for bilayer formation.

Contact between droplets provides a bridge and can help with interdroplet contact. Osmotic pressure and a thermodynamic force drive the diffusional flux of molecules through the membrane. Thus, they are reasons for the transfer in the case of some chemical compounds.[13,18,23]

Droplet systems must meet specific criteria to be used in biological research. Primarily, emulsions must be stabilized against coalescence by adding surfactants. Furthermore, the continuous liquid must be inert and allow for the transport of gas to the droplets. These requirements are conveniently satisfied by the use of fluorinated oil as a continuous liquid.[24,25] The oil is typically enriched with biologically inert nonionic triblock fluorosurfactants (i.e., $(PFPE)_2PEG$ copolymers), both compliant with the previously mentioned conditions.[26,27] The final fundamental requirement is that the droplets present a barrier to the transport of chemical ingredients. Recent studies report molecular transport between droplets, raising highly relevant questions about the compatibility of droplet-based systems with AST.[13,14] First, emulsions are metastable and prone to destruction in some conditions. Aging processes like coalescence or Ostwald ripening occur naturally in emulsions.[15,28,29] Moreover, most physiological environments are characterized by higher salt concentrations. As demonstrated in the literature, the stabilization of droplets by poly(ethylene glycol) PEG-bond surfactants decreases with increasing droplet salinity.[16,30]

Considering all observations mentioned above, the magnitude of transport of small molecules for droplets and between droplets may depend significantly on the characteristics of these molecules. While controlling the retention of active compounds is the key to the use of droplet systems in analytical studies, the transport so far has been tracked with the use of model fluorophores.[13,14,21,23,31−34] Unfortunately, most antimicrobials are not fluorescent or very weakly fluorescent. However, differences in chemical structures between antibiotics and fluorophores exclude the possibility of comparing them. Working on new nonleaking surfactants, Chowdhury et al. used a cell-based reporter system to detect the transfer of nonfluorescent molecules of doxycycline. The signal from green fluorescent protein (GFP) in HEK 293 cells in this study has been induced by the inflow of the antimicrobial agent.[31,35,36] An increase in the fluorescence signal allowed indirect observation and aided in tracking the transport of antibiotics to cell-loaded droplets. Nevertheless, this study was limited to only one type of antibiotic. Here, we expand on this approach and demonstrate how physicochemical properties predict the retention or the interdroplet transport of small, nonfluorescent molecules. We verify the prediction by screening the array of antibiotics for their leakage in such droplet systems.

EXPERIMENTAL SECTION

Bacteria. The fluorescent strain of *Escherichia coli* Top10 placEGFP was obtained from Prof. Weibel's group, the Department of Biochemistry, University of Wisconsin, Madison. Before each experiment, bacteria were incubated on Luria−Miller agar (Roth, Germany) plates with the addition of 100 μg/mL ampicillin sodium salt (Sigma-Aldrich, Germany). After incubation, a colony of bacteria was inoculated in a liquid Mueller−Hinton medium (Roth, Germany) with 100 μg of ampicillin and incubated overnight. After incubation, we diluted the bacteria with the fresh medium until they reached an optical density of 0.1, representing around 10^8 CFU/mL. In our experiments, we always encapsulated around 10 bacterial cells per droplet (control samples always stayed contained above 85% of positive droplets).

Antibiotics. Stock solutions of kanamycin sulfate (Fisher Chemical, U.K.), cefotaxime sodium salt (Roth, Germany), gentamycin sulfate (Toku-E), spectinomycin dihydrochloride pentahydrate (Roth, Germany), tetracycline hydrochloride (Roth, Germany), doxycycline hyclate (Roth, Germany), ceftazidime pentahydrate (Acros Organics, Belgium), amikacin sulfate (Toku-E), tobramycin sulfate (Toku-E), fosfomycin sulfate (Toku-E), imipenem (Toku-E), and meropenem (Toku-E) were dissolved in distilled water. Chloramphenicol (Toku-E) and levofloxacin (Toku-E) were dissolved in 50% ethanol. Norfloxacin (Toku-E) was dissolved in 5% acetic acid (POCH, Poland). Ciprofloxacin (Toku-E) was dissolved in 0.1 M NaOH (POCH, Poland). Trovafloxacin mesylate (Sigma, Germany) and nitrofurantoin (Toku-E) were dissolved in DMSO (Roth, Germany). We determined the minimal inhibitory concentrations (MICs) of testing antibiotics by the standard broth dilution method. After overnight incubation on 96-well plates, we estimated MIC values: 1.5 μg/mL kanamycin, 0.64 μg/mL cefotaxime, 0.75 μg/mL gentamycin, 3 μg/mL spectinomycin, 1.5 μg/mL tetracycline, 0.5 μg/mL doxycycline, 1 μg/mL chloramphenicol, 0.02 μg/mL norfloxacin, 0.006 μg/mL ciprofloxacin, 0.004 μg/mL levofloxacin, 4 μg/mL amikacin, 4 μg/mL fosfomycin, 0.004 μg/mL trovafloxacin, 1 μg/mL ceftazidime, 1.5 μg/mL tobramycin, 0.75 μg/mL imipenem, 0.1 μg/mL meropenem, and 3 μg/mL nitrofurantoin.

Microfluidic Chips. We used two microfluidic chips for (i) the generation of droplets and (ii) detection (Figures S1 and S2). Both devices were made of poly(dimethyl siloxane) (PDMS; Sylgard silicone elastomer kit, Dow Corning) and manufactured by the same procedure. In the first step, we fabricated molds from polycarbonate (PC) (Macroclear, Bayer, Germany) using a CNC milling machine (MSG4025, Ergwind, Poland). Next, we prepared PDMS negative masters by pouring PDMS on a PC chip. PDMS polymerized during incubation at 95 °C for 45 min. Then, we removed the PC chip and silanized the PDMS mold with the use of tridecafluoro-1,1,2,2-tetrahydrooctyl-1-trichlorosilane (United Chemical Technologies) for 3 h under 10 mbar pressure with vapors. We prepared PDMS replicas by pouring PDMS on silanized negative masters and incubating them at 95 °C for 45 min. We bound PDMS replicas with glass slides by exposing them to oxygen plasma. Before use, channels in chips were hydrophobically modified by filling the chip with Novec 1720 (3M).

https://doi.org/10.1021/acs.analchem.2c04644
Anal. Chem. 2023, 95, 1574−1581

Scheme 1. Color-Coded Method for the Indirect Analysis of Antibiotic Leakage in Droplets[a]

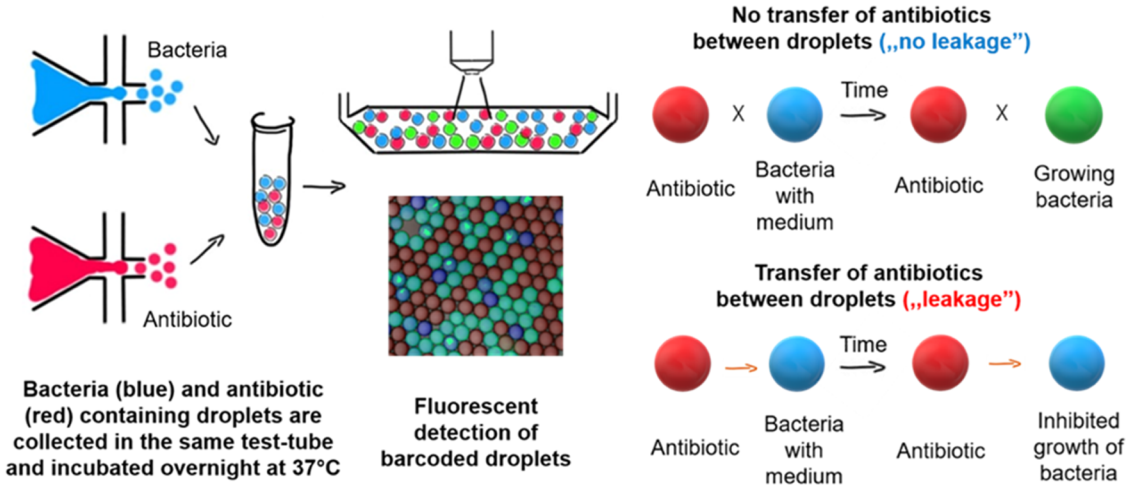

[a]We generated and mixed two samples with droplets. We labeled droplets with bacteria with a blue fluorescent dye (Cascade Blue). We marked antibiotic-loaded droplets with a red fluorescent dye (Alexa Fluor). After overnight incubation (approximately 12−15 h), we injected droplet samples into a custom-made microfluidic detection chamber and captured images of 2D droplet monolayers by confocal microscopy. The viability of bacteria is estimated by measuring the intensity of green fluorescence from actively growing bacteria. The cross-talk (leakage) of antibiotics from droplets to neighboring bacteria-containing droplets inhibits bacteria growth and is verified by the emergence of fluorescent signals.

Droplet Generation and Incubation. In our method, we co-incubate two different groups of droplets. The first part of the emulsion consists of droplets with an antibiotic concentration 100 times higher than the minimal inhibitory concentration (MIC). We used antibiotics from different classes to generate 100× MIC droplets: (i) aminoglycosides: 150 μg/mL kanamycin (KAN), 400 μg/mL amikacin (AMK), 150 μg/mL tobramycin (TOB), and 75 μg/mL gentamycin (GEN); (ii) β-lactams: 64 μg/mL cefotaxime (CTX) and 100 μg/mL ceftazidime (CAZ); (iii) tetracyclines: 100 μg/mL tetracycline (TET) and 50 μg/mL doxycycline (DOX); (iv) fluoroquinolones: 2 μg/mL norfloxacin (NOR), 0.6 μg/mL ciprofloxacin (CIP), 0.4 μg/mL levofloxacin (LVX), and 0.4 μg/mL trovafloxacin (TVA); and (v) other antibiotics: 300 μg/mL spectinomycin (SPT), 100 μg/mL chloramphenicol (CHL), and 400 μg/mL fosfomycin (FOF). We added red fluorescent dye Alexa Fluor (Invitrogen) at a concentration of 6 mg/L to recognize this group of droplets.

Additionally, we generated a second part of the emulsion, consisting of droplets with *E. coli* expressing green fluorescent protein (around 10 cells per droplet). We labeled this portion of droplets with 2 mg/L blue fluorescent Cascade Blue (Invitrogen). Bacteria-loaded droplets have high green fluorescence signals only after multiple replications of living cells. Antibiotic migration from neighbor droplets inhibits bacterial replication, and droplets remain fluorescent only in the blue color. If the transfer of antimicrobials does not occur in the emulsion, then bacteria actively grow and produce a strong green fluorescent signal (Scheme 1).

We detected the fluorescence of droplets after incubation. We imaged droplets at three different wavelengths: (i) 405 nm for Cascade Blue, (ii) 488 nm for GFP produced by actively growing bacteria, and (iii) 635 nm for Alexa Fluor. We determined the intensities of green fluorescence from a blue-coded population of droplets and compared it with the control experiments (bacteria co-incubated with blank droplets without antibiotics) (Figure S5). Irregular droplets with no matched coding and size were excluded from the data analysis. In our experiments, we did two repetitions with two commonly used surfactants: (i) $(PFPE)_2PEG$ (manufactured by our group, Poland) and (ii) FluoSurf N (Emulseo, France). $(PFPE)_2PEG$ is a nonionic triblock fluorosurfactant. FluoSurf N is a mixture of diblock and triblock polymers (PFPE-b-PPO-PEO-PPO-b-PFPE) with a molecular weight ranging from 7 to 13kD. We did not see significant differences between the results for these two surfactants; therefore, we treated both experiments as duplicates (Figure S3).

Detection Software. An inverted fluorescence microscope in the epi-configuration was used to acquire images of the droplets in three channels: red, green, and blue (RGB). Software was customized to automate the reading of the intensity for many experiments and facilitate the analysis of the obtained results and was supported with the ImageJ particle analysis module.[37] We determined the areas occupied by the droplets with bacteria by analyzing the image from the blue channel, and then we determined the fluorescence intensity from the green channel. The red channel was omitted since all red-labeled droplets served only as cargo for antibiotics and did not contain reporter cells.

Data Analysis. All chemical descriptors were calculated with the use of the .NET Chemistry Development Kit (NCDK),[38] which is the .NET Framework port of The Chemistry Development Kit (CDK). The CDK is a commonly used open-source library for chemo- and bioinformatics.[39−41] We created our program (using C# programming language) for the NCDK library maintenance to improve the computing of chemical descriptors. NCDK calculates X log *P* (partition coefficient) and PSA (polar surface area) according to algorithms described in the literature.[42−44] The correlation between descriptors and experimentally tested leakage was calculated using the Pearson correlation coefficient. We applied the *k*-means algorithm to assign antibiotics to the appropriate cluster (leaky or nonleaky cluster). Both Pearson correlation and *k*-means were calculated using Origin 2020b (Figures S7−S9).

https://doi.org/10.1021/acs.analchem.2c04644
Anal. Chem. 2023, 95, 1574−1581

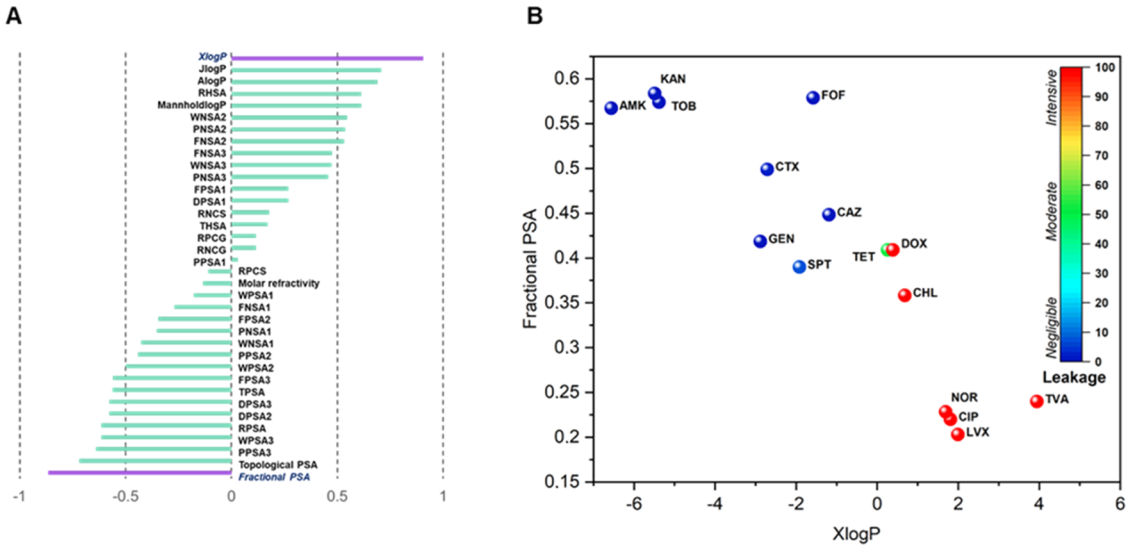

Figure 2. X log *P* and fractional PSA are in the best correlation with the experimentally determined leakage of antibiotics. (A) Pearson correlation between the leakage values and 36 different chemical descriptors. Descriptors with a correlation close to 1/−1 are the best descriptors for the classification of antibiotics into leaky or nonleaky groups. (B) Dependence of X log *P* and fractional PSA values on the ability to leak for 15 tested antibiotics.

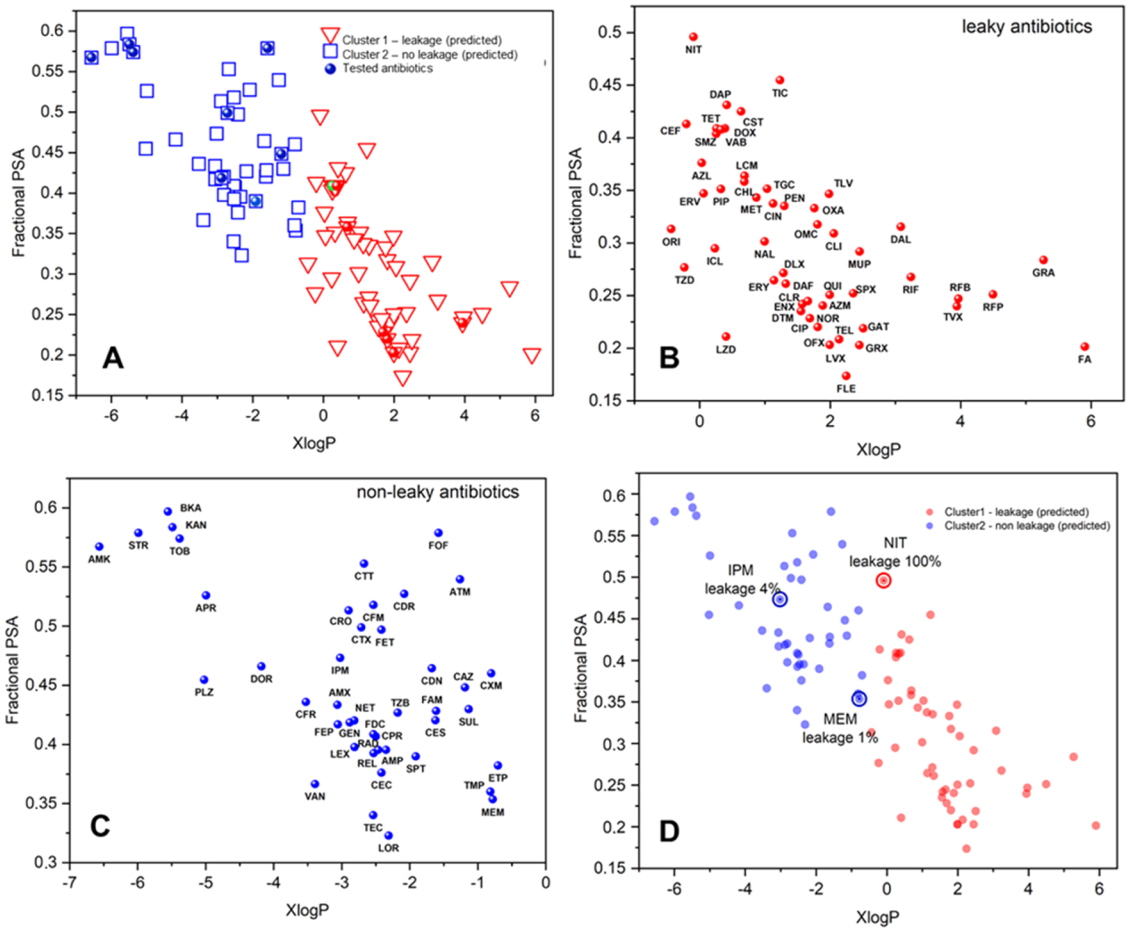

Figure 3. Leakage of antimicrobials depends on X log *P* and fractional PSA values. (A) Theoretical prediction of the antibiotics' cross-talk between droplets. We defined leakage values as a percentage decrease in the viability of bacteria incubated with the companion of antibiotics. X log *P* and fractional PSA descriptors correlate with the leakage rates of tested antibiotics. We used a *k*-means plot to separate leaky and nonleaky groups of antibiotics. (B) Predicted group of leaking antibiotics. (C) Predicted group of nonleaky antibiotics. (D) Experimental data for the three selected antibiotics (NIT, IPM, and MEM) agree with the prediction.

https://doi.org/10.1021/acs.analchem.2c04644
Anal. Chem. 2023, 95, 1574−1581

RESULTS AND DISCUSSION

We observed two distinctly recognizable responses of bacterial populations co-incubated with antibiotic-loaded droplets. For certain antibiotics, there was a significant decrease in the fluorescence of bacteria in droplets (weak green signal), which we associate with the cross-talk of antibiotics between droplets. The other group of antibiotics did not decrease the fluorescence of bacteria in accompanying emulsions (intensive green signal). We define leakage as a percentage of bacterial growth inhibition caused by the transfer of antibiotics to droplets with encapsulated bacteria. Antibiotics that did not cause antagonistic effects on the incubated bacterial population (leakage rates from 0−60%) are AMK, TOB, KAN, CTX, GEN, SPT, FOF, and CAZ. The highest leakage rates (above 60%) were observed in samples with DOX, CHL, NOR, CIP, LVX, and TVA. With a leakage rate of 52%, only TET manifests the average inhibition of the viability of bacteria.

The findings of the significant transfer of antimicrobials between droplets in this particular complex emulsion prompted us to search further for the link between the chemical nature of these antibiotics and their leakage. In the first step of searching for clues into how the structure of an antibiotic influences its cross-talk between droplets, we decided to screen the physicochemical parameters of antimicrobial molecules. We focused mainly on those concerning the hydrophilic/hydrophobic nature of the molecules, i.e., partition coefficients, also referred to as X log *P*, and descriptors describing the nature of the molecule's surface. We calculated 36 different parameters and estimated their correlation with the experimental data on the leakage of antimicrobials (Figure S8). After extensive analysis of all of the descriptors, we concluded that X log *P* and fractional PSA offer the best correlation with antibiotic leakage rates (Figure 2). The partition coefficient defines the ratio of the concentrations of two immiscible component systems in an equilibrium state. Small molecules with a high X log *P* (hydrophobic nature) will more likely escape from aqueous phases into the hydrophobic phase. Fractional polar surface area is one of the parameters that describe the polarity of chemical compounds (including the molecular size of the compound).

Our next step was to estimate if using these two descriptors will determine whether the antibiotic will leak out the droplets with a higher or lower probability. Our data set contained X log *P* and fractional PSA values of 95 different antibiotics (Figure S9). To recognize two groups of antimicrobial escape, we use the *k*-means algorithm. This algorithm determines clusters within an unlabeled multidimensional data set (Figure 3).

To confirm the prediction that X log *P* and PSA are the key properties, we repeated experiments with three randomly chosen antibiotics: (i) 75 μg/mL imipenem (IPM), (ii) 10 μg/mL meropenem (MEM), and (iii) 300 μg/mL nitrofurantoin (NIT). Only NIT shows a significant leakage confirming a decrease in bacterial viability. The bacterial population remained undisturbed after co-incubation with IPM and MEM. This experimental data fits the predicted results (Figure 3D). We investigated how similar the retention characteristics are within antibiotics and if this can be used to predict the cross-talk of antibiotics in water-in-oil systems (Figure 4). For that, we plotted the same X log *P* values against FPSA and labeled antibiotic classes differently. Here, we used the antibiotic classes that had at least four representatives in our study. We saw that in many cases, the knowledge of the antibiotic class alone was sufficient to determine the potential cross-talk. All aminoglycosides were positioned in the nonleaky part of the plot, while all (fluoro)quinolones, tetracyclines, and macrolides were leaky. Note: in our study, we included ansamycins also under the macrolides. β-lactams and glycopeptides had both leaky and nonleaky antibiotics present. β-lactams had the most representatives in our study, so we looked deeper into the retention behavior of their subclasses. Carbapenems and most of the cephems were nonleaky, while most of the penicillins showed potentially leaky parameters.

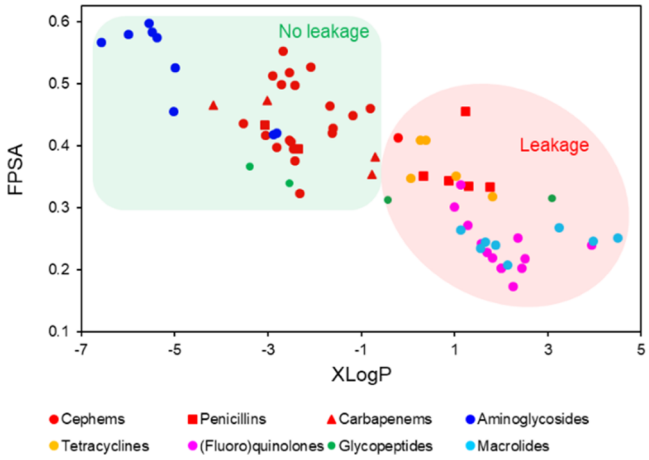

Figure 4. Antibiotic class or subclass predicts the retention characteristics of the antibiotics in most cases. The partition coefficient (X log *P*) is on the *X*-axis and the fractional polar surface area (FPSA) is on the *y*-axis. With the green background, we show antibiotics that are most likely to be retained in water-in-oil droplets, while with the red background, we show potentially leaky antibiotics. Aminoglycosides (blue dots) and β-lactam subclasses carbapenems and most of the cephems (red triangles and dots) remain in droplets. β lactam penicillins (red squares), tetracyclines (yellow dots), (fluoro)quinolones (purple dots), and macrolides (light blue dots) are most likely all leaky types. Glycopeptides (green dots) and penicillins (red squares) have both leaky and nonleaky antibiotics.

Distance and Mixing-Related Transfer of Antibiotics. We generated droplets with two antibiotics previously observed to leak (NOR and LVX) and droplets with bacteria to test the hypothesis that direct contact of droplets accelerates antibiotic transfer (Figure S6). For this, we prepared three different groups of samples. The first group was prepared according to the standard protocol described above−droplets with 100× MIC of antibiotics and droplets with bacteria. After generation, we mixed droplets thoroughly right before incubation. The second sample was not mixed, resulting in two ordered layers of droplets with different contents (encapsulated layer of antibiotics and the layer with bacteria). Usually, when introducing the second type of droplet, the tip of the Teflon tube is immersed in an oil phase (well below the first droplet layer). The buoyant droplets settle at the bottom of the first layer, giving rise to a second layer. Given the small diameter of the Eppendorf tube, droplets in these two layers have minimal freedom to move or intermix. Hence, contact of droplets with the different compositions is generally limited to the interface of the two layers. This may affect the outcome of the measurements. The third sample group was separated with a 15 μL layer of empty droplets labeled with a low concentration (1 mg/L) of Alexa Fluor (Figure 5). After overnight incubation, the droplets were scanned and the

https://doi.org/10.1021/acs.analchem.2c04644
Anal. Chem. 2023, 95, 1574−1581

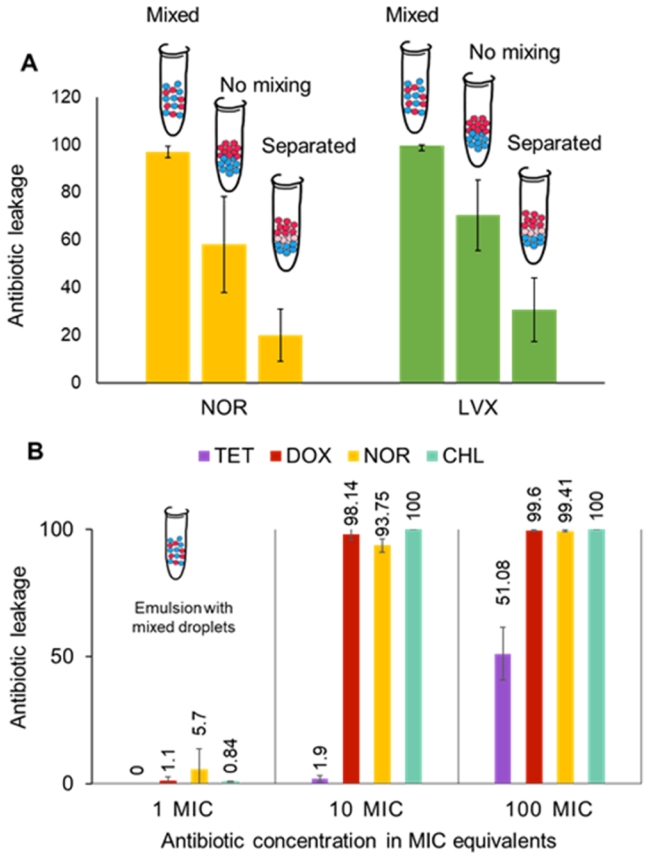

Figure 5. Cross-talk of antimicrobials between droplets is accelerated by the concentration and direct contact with neighboring droplets. (A) Transfer of antibiotics between droplets is fast along the concentration gradient with properly mixed droplets. We observed the most significant loss of bacterial viability in droplets when emulsions of antibiotics and bacteria were adequately mixed and were in close proximity. Emulsions that were not mixed or had a separating layer of blank droplets (growth medium) presented a higher viability of bacteria than well-mixed emulsions and (B) antibiotic leakage between droplets is concentration-dependent. Incubation with higher concentrations of antimicrobials results in lower rates of bacterial viability. Transfer of antibiotics from droplets with concentrations around 1× MIC is slow and does not result in a sharp decrease in viability in the case of tested antibiotics.

leakage-related decrease in the viability of bacteria from different preparation groups was compared. We observed a significant decrease in antibiotic transfer in nonmixed and separated emulsions (Figure 5A). Thus, to avoid the cross-talk of antimicrobials between droplets with different chemical compositions, the different fractions of emulsions should be separated. Antimicrobials result in lower rates of bacterial viability. Transfer of antibiotics from droplets with concentrations around 1× MIC is slow and does not result in a sharp decrease in viability in the case of tested antibiotics.

Concentration-Dependent Transfer of Antibiotics. In further steps, we attempt to define the influence of concentration on the cross-talk rate of antibiotics. The concentration gradient between droplets can significantly affect the strength of the influx of antibiotics from droplet to droplet. As has been mentioned, we prepared samples with three different concentrations of antibiotics (100, 10, and 1× MIC). For this experiment, we tested only a few representatives of different antibiotic classes with the tendency to leak. We used the following concentrations of the antimicrobial agents: (i) 100, 10, and 1 μg/mL TET; (ii) 50, 5, and 0.5 μg/mL DOX; (iii) 100, 10, and 1 μg/mL CHL; and (iv) 2, 0.2, and 0.02 μg/mL NOR (Figure S5). As in previous experiments, we used our detection chamber to measure the fluorescence intensity of droplets with bacteria.

We found that the transport of antimicrobials is very efficient and occurs even in 10x MIC concentrations. We did not observe any leakage-related decrease in bacterial viability in emulsions with the lowest antibiotic concentrations (1× MIC). Diluting a small amount of the antibiotic may compensate for its harmful effect on bacteria but does not exclude its transport, even at a minimal rate (Figure 5B).

CONCLUSIONS

Microfluidics is a powerful tool in antibiotic resistance research. Still, there are important outstanding challenges in the adoption of droplet techniques. Deepening the understanding of the retention of active compounds in aqueous droplets and optimization of microfluidic systems is crucial for broadening the range of applications of this technology. One of the research assumptions of droplet microbioreactors is to ensure stable conditions for chemical reactions and biological processes. The results obtained by the microfluidic method must correlate with studies conducted on a macroscale and be aligned with the universal clinical guidelines (i.e., European Committee on Antimicrobial Susceptibility Testing EUCAST recommendations). Every microbioreactor must maintain its chemical stability and not leak or take up the components of the assay. In our study, we have demonstrated a novel method to find the chemical factors that accelerate the escape of nonfluorescent reagents from droplets. We have found that there are two highly different leakage properties of antimicrobials. The analysis of chemical descriptors concerning the hydrophilic/hydrophobic nature of the molecules has shown that two of them, partition coefficient and fractional polar surface area, offer a good correlation with experimental data and thus a predictor for retention inside droplets. Our research is designed to understand and avoid the factors influencing the results of experiments in microfluidic emulsions. We hope that our work will open an earnest discussion on the validity of experiments performed using two-phase microfluidic systems.

ASSOCIATED CONTENT

Supporting Information

The Supporting Information is available free of charge at https://pubs.acs.org/doi/10.1021/acs.analchem.2c04644.

Scheme of the droplet generation chip (Figure S1); scheme of the detection chamber (Figure S2); viability values (Table S1); histograms with the intensity of fluorescence (Figures S3−S5); software design (Figure S5); Pearson correlation coefficient values and list of descriptors (Table S2); and X log *P* and fPSA values (Table S3) (PDF)

AUTHOR INFORMATION

Corresponding Authors

Piotr Garstecki − *Institute of Physical Chemistry, Polish Academy of Sciences, 01-224 Warsaw, Poland;* orcid.org/0000-0001-9101-7163; Email: garst@ichf.edu.pl

https://doi.org/10.1021/acs.analchem.2c04644
Anal. Chem. 2023, 95, 1574−1581

Ott Scheler − *Department of Chemistry and Biotechnology, Tallinn University of Technology (TalTech), Tallinn 12618, Estonia;* orcid.org/0000-0002-8428-1350; Email: ott.scheler@taltech.ee

Authors

Artur Ruszczak − *Institute of Physical Chemistry, Polish Academy of Sciences, 01-224 Warsaw, Poland*

Paweł Jankowski − *Institute of Physical Chemistry, Polish Academy of Sciences, 01-224 Warsaw, Poland*

Shreyas K. Vasantham − *Institute of Physical Chemistry, Polish Academy of Sciences, 01-224 Warsaw, Poland*

Complete contact information is available at: https://pubs.acs.org/10.1021/acs.analchem.2c04644

Author Contributions

§A.R. and P.J. contributed equally to this work; A.R. collected all experimental data; P.J. carried out antibiotic descriptor characterization and designed the software for the detection; S.K.V. assisted in microfluidic chip design and optical setup; and P.G. and O.S. helped in conceptualizing the study. The manuscript was written through the contributions of all authors. All authors have approved the final version of the manuscript.

Notes

The authors declare no competing financial interest.

■ ACKNOWLEDGMENTS

Funding for this research was provided by the National Science Centre, Poland, funding based on decision 2018/30/A/ST4/00036, Maestro 10. O.S. acknowledges support from the Estonian Research Council grants MOBTP109 and PRG620 and from the TTU Development Program 2016−2022 (project no. 2014-2020.4.01.16.0032). S.K.V. acknowledges support from the Foundation for Polish Science TEAM NET POIR.04.04.00-00-16ED/18-00.

■ REFERENCES

(1) Churski, K.; Kaminski, T. S.; Jakiela, S.; Kamysz, W.; Baranska-Rybak, W.; Weibel, D. B.; Garstecki, P. *Lab Chip* **2012**, *12*, 1629−1637.
(2) Jakiela, S.; Kaminski, T. S.; Cybulski, O.; Weibel, D. B.; Garstecki, P. *Angew. Chem., Int. Ed.* **2013**, *52*, 8908−8911.
(3) Jian, X.; Guo, X.; Wang, J.; Tan, Z. L.; Xing, X. H.; Wang, L.; Zhang, C. *Biotechnol. Bioeng.* **2020**, *117*, 1724−1737.
(4) Kaminski, T. S.; Scheler, O.; Garstecki, P. *Lab Chip* **2016**, *16*, 2168−2187.
(5) Takeuchi, S.; Garstecki, P.; Weibel, D. B.; Whitesides, G. M. *Adv. Mater.* **2005**, *17*, 1067−1072.
(6) Whitesides, G. M. *Nature* **2006**, *442*, 368−373.
(7) Baekkeskov, E.; Rubin, O.; Munkholm, L.; Zaman, W. *Antimicrobial Resistance as a Global Health Crisis*; Oxford University Press, 2020.
(8) Jankowski, P.; Kutaszewicz, R.; Ogończyk, D.; Garstecki, P. *J. Flow Chem.* **2020**, *10*, 397−408.
(9) Matuła, K.; Rivello, F.; Huck, W. T. S. *Adv. Biosyst.* **2020**, *4*, No. 1900188.
(10) Hsu, R. H.; Clark, R. L.; Tan, J. W.; Ahn, J. C.; Gupta, S.; Romero, P. A.; Venturelli, O. S. *Cell Syst.* **2019**, *9*, 229−242.
(11) Postek, W.; Gargulinski, P.; Scheler, O.; Kaminski, T. S.; Garstecki, P. *Lab Chip* **2018**, *18*, 3668−3677.
(12) Scheler, O.; Makuch, K.; Debski, P. R.; Horka, M.; Ruszczak, A.; Pacocha, N.; Sozanski, K.; Smolander, O. P.; Postek, W.; Garstecki, P. *Sci. Rep.* **2020**, *10*, No. 3282.
(13) Gruner, P.; Riechers, B.; Semin, B.; Lim, J.; Johnston, A.; Short, K.; Baret, J.-C. *Nat. Commun.* **2016**, *7*, No. 10392.
(14) Etienne, G.; Vian, A.; Biočanin, M.; Deplancke, B.; Amstad, E. *Lab Chip* **2018**, *18*, 3903−3912.
(15) Weiss, J.; Canceliere, C.; McClements, D. J. *Langmuir* **2000**, *16*, 6833−6838.
(16) Etienne, G.; Kessler, M.; Amstad, E. *Macromol. Chem. Phys.* **2017**, *218*, No. 1600365.
(17) Debon, A. P.; Wootton, R. C.; Elvira, K. S. *Biomicrofluidics* **2015**, *9*, No. 024119.
(18) Thiam, A. R.; Bremond, N.; Bibette, J. *Langmuir* **2012**, *28*, 6291−6298.
(19) Payne, E. M.; Holland-Moritz, D. A.; Sun, S.; Kennedy, R. T. *Lab Chip* **2020**, *20*, 2247−2262.
(20) Chen, Y.; Wijaya Gani, A.; Tang, S. K. *Lab Chip* **2012**, *12*, 5093−5103.
(21) Scheler, O.; Kaminski, T. S.; Ruszczak, A.; Garstecki, P. *ACS Appl. Mater. Interfaces* **2016**, *8*, 11318−11325.
(22) Kulesa, A.; Kehe, J.; Hurtado, J. E.; Tawde, P.; Blainey, P. C. *Proc. Natl. Acad. Sci. U.S.A.* **2018**, *115*, 6685−6690.
(23) Skhiri, Y.; Gruner, P.; Semin, B.; Brosseau, Q.; Pekin, D.; Mazutis, L.; Goust, V.; Kleinschmidt, F.; El Harrak, A.; Hutchison, J. B.; et al. *Soft Matter* **2012**, *8*, 10618−10627.
(24) Ki, S.; Kang, D. K. *Biosensors* **2020**, *10*, No. 172.
(25) Horka, M.; Sun, S.; Ruszczak, A.; Garstecki, P.; Mayr, T. *Anal. Chem.* **2016**, *88*, 12006−12012.
(26) Holtze, C.; Rowat, A. C.; Agresti, J. J.; Hutchison, J. B.; Angile, F. E.; Schmitz, C. H.; Koster, S.; Duan, H.; Humphry, K. J.; Scanga, R. A.; et al. *Lab Chip* **2008**, *8*, 1632−1639.
(27) Chiu, Y.-L.; Chan, H. F.; Phua, K. K. L.; Zhang, Y.; Juul, S.; Knudsen, B. R.; Ho, Y.-P.; Leong, K. W. *ACS Nano* **2014**, *8*, 3913−3920.
(28) Ariyaprakai, S.; Dungan, S. R. *J. Colloid Interface Sci.* **2010**, *343*, 102−108.
(29) Gupta, A.; Eral, H. B.; Hatton, T. A.; Doyle, P. S. *Soft Matter* **2016**, *12*, 2826−2841.
(30) Malisova, B.; Tosatti, S.; Textor, M.; Gademann, K.; Zürcher, S. *Langmuir* **2010**, *26*, 4018−4026.
(31) Chowdhury, M. S.; Zheng, W.; Kumari, S.; Heyman, J.; Zhang, X.; Dey, P.; Weitz, D. A.; Haag, R. *Nat. Commun.* **2019**, *10*, No. 4546.
(32) Janiesch, J. W.; Weiss, M.; Kannenberg, G.; Hannabuss, J.; Surrey, T.; Platzman, I.; Spatz, J. P. *Anal. Chem.* **2015**, *87*, 2063−2067.
(33) Najah, M.; Mayot, E.; Mahendra-Wijaya, I. P.; Griffiths, A. D.; Ladame, S.; Drevelle, A. *Anal. Chem.* **2013**, *85*, 9807−9814.
(34) Courtois, F.; Olguin, L. F.; Whyte, G.; Theberge, A. B.; Huck, W. T. S.; Hollfelder, F.; Abell, C. *Anal. Chem.* **2009**, *81*, 3008−3016.
(35) Chowdhury, M. S.; Zhang, X.; Amini, L.; Dey, P.; Singh, A. K.; Faghani, A.; Schmueck-Henneresse, M.; Haag, R. *Nano-Micro Lett.* **2021**, *13*, No. 147.
(36) Chowdhury, M. S.; Zheng, W.; Singh, A. K.; Ong, I. L. H.; Hou, Y.; Heyman, J. A.; Faghani, A.; Amstad, E.; Weitz, D. A.; Haag, R. *Soft Matter* **2021**, *17*, 7260−7267.
(37) Schneider, C. A.; Rasband, W. S.; Eliceiri, K. W. *Nat. Methods* **2012**, *9*, 671−675.
(38) Ujihara, K. *NCDK -.NET Libraries for Cheminformatics*. 2018. https://kazuyaujihara.github.io/NCDK/html/e2ff06cc-99b7-4f8b-95c5-53965548639f.htm.
(39) Steinbeck, C.; Han, Y.; Kuhn, S.; Horlacher, O.; Luttmann, E.; Willighagen, E. *J. Chem. Inf. Comput. Sci.* **2003**, *43*, 493−500.
(40) Steinbeck, C.; Hoppe, C.; Kuhn, S.; Floris, M.; Guha, R.; Willighagen, E. L. *Curr. Pharm. Des.* **2006**, *12*, 2111−2120.
(41) Willighagen, E. L.; Mayfield, J. W.; Alvarsson, J.; Berg, A.; Carlsson, L.; Jeliazkova, N.; Kuhn, S.; Pluskal, T.; Rojas-Cherto, M.; Spjuth, O.; et al. *J. Cheminf.* **2017**, *9*, No. 33.
(42) Wang, R.; Gao, Y.; Lai, L. *Perspect. Drug Discovery Des.* **2000**, *19*, 47−66.
(43) Wang, R. X.; Fu, Y.; Lai, L. H. *J. Chem. Inf. Comput. Sci.* **1997**, *37*, 615−621.

(44) Ertl, P.; Rohde, B.; Selzer, P. *J. Med. Chem.* **2000**, *43*, 3714−3717.

https://doi.org/10.1021/acs.analchem.2c04644
Anal. Chem. 2023, 95, 1574−1581